Monitoring the Long-Term Degradation Behavior of Biomimetic Bioadhesive using Wireless Magnetoelastic Sensor

Meng-Hsien Lin [students],
Department of Biomedical Engineering, Michigan Technological University, Houghton, MI 49931 USA

Jonathan Anderson [students],
Department of Biomedical Engineering, Michigan Technological University, Houghton, MI 49931 USA

Rattapol Pinnaratip [students],
Department of Biomedical Engineering, Michigan Technological University, Houghton, MI 49931 USA

Hao Meng [students],
Department of Biomedical Engineering, Michigan Technological University, Houghton, MI 49931 USA

Shari Konst [student],
Department of Chemistry, Michigan Technological University, Houghton, MI 49931 USA

Andrew J. DeRouin [students],
Department of Biomedical Engineering, Michigan Technological University, Houghton, MI 49931 USA

Rupak Rajachar [professors],
Department of Biomedical Engineering, Michigan Technological University, Houghton, MI 49931 USA

Keat Ghee Ong [professors], and
Department of Biomedical Engineering, Michigan Technological University, Houghton, MI 49931 USA

Bruce P. Lee [professors]
Department of Biomedical Engineering, Michigan Technological University, Houghton, MI 49931 USA

Meng-Hsien Lin: mlin1@mtu.edu; Jonathan Anderson: jjander1@mtu.edu; Rattapol Pinnaratip: rpinnara@mtu.edu; Hao Meng: haom@mtu.edu; Shari Konst: smkonst@mtu.edu; Andrew J. DeRouin: ajderoui@mtu.edu; Rupak Rajachar: rupakr@mtu.edu; Keat Ghee Ong: kgong@mtu.edu; Bruce P. Lee: bplee@mtu.edu

Abstract

Correspondence to: Keat Ghee Ong, kgong@mtu.edu; Bruce P. Lee, bplee@mtu.edu.

The degradation behavior of a tissue adhesive is critical to its ability to repair a wound while minimizing prolonged inflammatory response. Traditional degradation tests can be expensive to perform, as they require large numbers of samples. The potential for using magnetoelastic resonant sensors to track bioadhesive degradation behavior was investigated. Specifically, biomimetic poly(ethylene glycol)- (PEG-) based adhesive was coated onto magnetoelastic (ME) sensor strips. Adhesive-coated samples were submerged in solutions buffered at multiple pH levels (5.7, 7.4 and 10.0) at body temperature (37°C) and the degradation behavior of the adhesive was tracked wirelessly by monitoring the changes in the resonant amplitude of the sensors for over 80 days. Adhesive incubated at pH 7.4 degraded over 75 days, which matched previously published data for bulk degradation behavior of the adhesive while utilizing significantly less material ($\sim 10^3$ times lower). Adhesive incubated at pH 10.0 degraded within 25 days while samples incubated at pH 5.7 did not completely degrade even after 80 days of incubation. As expected, the rate of degradation increased with increasing pH as the rate of ester bond hydrolysis is higher under basic conditions. As a result of requiring a significantly lower amount of samples compared to traditional methods, the ME sensing technology is highly attractive for fully characterizing the degradation behavior of tissue adhesives in a wide range of physiological conditions.

Index Terms

Magnetoelastic sensor; biodegradation; mussel adhesive protein; tissue adhesive

I. Introduction

Tissue adhesives are universally applied in surgeries [1–3]. The ability to control the degradation rate of the adhesive is critical to the success of its application. The adhesive needs to maintain its mechanical integrity to prevent premature rupture of the repaired wound. However, the prolonged presence of the adhesive can act as a barrier for the union of the wound edges. Thus, the rate of degradation for an adhesive must be tailored to match the rate of tissue ingrowth as the wound heals.

While the pH of oxygenated blood and internal organs ranges from 7.2 to 7.45 [4, 5], the pH levels of skin (pH = 4–6) [6], subcutaneous tissues (pH = 6.7–7.1) [7], tumor tissues (pH < 6.9) [8], and internal tissues after prolonged hemorrhage (pH < 7) [9, 10] are more acidic. Therefore, there is a need to characterize the degradation behavior of tissue adhesives under multiple conditions to better mimic various physiological environments. This requires a significant number of sets of experiments to characterize a sample. Unfortunately, today the typical characterization of the degradation behavior for tissue adhesives still involves tracking the mass loss of the adhesive over time [11, 12], which utilizes a large amount of sample. The need for a large quantity of material required for traditional degradation testing makes it cost prohibitive to conduct comprehensive studies to evaluate the effects of multiple factors on the degradation behavior of bioadhesives. Additionally, these experiments are performed under simulated physiological conditions and may not reflect the complex environment and foreign body response that an adhesive would experience in the

body. Currently, no accurate methods exist for quantitatively monitoring the *in vivo* biodegradation behavior of tissue adhesives.

Recently, we reported the use of magnetoelastic (ME) sensors to track the degradation behavior of a fast degrading tissue adhesive over a period of several hours [13]. ME sensors are made of magnetoelastic materials, such as Metglas 2826MB ($Fe_{40}Ni_{38}Mo_4B_{18}$). Due to their large magnetoelastic coupling factor (~0.98) and a magnetostriction on the order of 10^{-5} [14–16], the Metglas-based ME sensor exhibits vibrations when excited by a magnetic AC field. At the resonant frequency of the ME sensor, the vibration also generates a significant magnetic field that can be remotely detected by capturing with a coil antenna [17]. When a mass is applied on the sensor surface, it causes a change in the resonant frequency and amplitude. In addition, the resonant frequency and amplitude of the sensor are sensitive to the elasticity of the applied coating or the viscosity of its surrounding medium. The ability to wirelessly monitor the change in mass or elasticity/viscosity allows the ME sensor to detect chemical and biological agents [18, 19] and material viscosity [20, 21]. Specifically, with proper surface functionalization, the ME sensor can be applied in cell culture or even implanted *in vivo* to monitor biointerfacial binding events, such as cellular attachment and proliferation [22, 23]. The remote query capability, as well as long-term durability of functionalized ME sensors in a biological environment, make them suitable for monitoring adhesive degradation in real time. Furthermore, compared to the traditional methods, the described ME sensor technology requires a significantly lower volume of sample.

Here, the ability of the ME sensing technology to monitor the long-term degradation behavior of a slow degrading adhesive was evaluated over several months *in vitro*. A synthetic bioadhesive that mimics the strong water-resistant adhesive properties of mussel adhesive proteins (MAPs) was coated onto ME sensors. In nature, these proteins enable mussels to bind tightly to various wet surfaces such as rocks, ships, piers, and other natural or manmade structures [24, 25]. MAPs contain a large quantity of an unusual amino acid, 3,4-dihydroxyphenylalanine (DOPA), which is believed to function as a crosslinking precursor and interfacial binding adhesive moiety [26, 27]. Various synthetic mimics of MAPs have demonstrated promise in functioning as tissue sealant [28, 29], an adhesive for soft tissue repair [30, 31], cell engineering [32, 33], drug delivery carriers [34], and antifouling coatings [35–37].

In this study, we employed a 4-armed poly(ethylene glycol) (PEG) end-modified with glutaric acid and dopamine (PEG-D; Figure 1) with known degradation rate [38]. PEG and the glutaric acid are linked by an ester bond, which undergoes hydrolysis with time. Dopamine consists of catechol group that mimics the adhesive and crosslinking properties of DOPA. PEG-D was spin-coated onto ME sensors and its degradation was monitored wirelessly in real time by tracking the changes in the resonant frequency and amplitude.

II. Experiments

A. Materials

3,4-dihydroxyphenethylamine hydrochloride (dopamine HCl) and sodium periodate ($NaIO_4$) were obtained from Acros Organics (Geel, Belgium). Phosphate buffered saline (PBS) and Tris HCl were obtained from Fisher Scientific (Fair Lawn, New Jersey). Parylene-C was obtained from Specialty Coating Systems Inc. (Indianapolis, IN). Metglas 2826MB ($Fe_{40}Ni_{38}Mo_4B_{18}$) was purchased from Metglas, Inc. (Conway, SC). PEG-D was synthesized following previously published protocol [39].

B. Preparing adhesive-coated sensor

PEG-D was coated onto ME sensor strips (12.7 mm × 5 mm × 30 μm) following previously published protocols with minor modifications (Figure 2) [13]. To prevent corrosion of the sensor surface in physiologically relevant aqueous buffers, ME sensor strips were first coated with Parylene-C to create a moisture barrier. Parylene-C is commonly used to generate an inert surface for various implantable medical devices such as pacemakers and defibrillators [40]. Additionally, Parylene-C-coated ME sensors were previously demonstrated to remain functional both in culture and *in vivo* [22, 41].

Sensor strips were coated with Parylene-C using a parylene deposition system (PDS 2010 Labcoter® 2, Special Coating Systems, Inc.) and then oxygen plasma (200 mTorr) etched (Jupiter II Reactive Ion Etcher, March Instruments) [22]. The sensors were then sonicated in ethanol for two minutes, rinsed with deionized (DI) water, and dried. The clean Parylene-C-coated sensors were submerged in a 10 mg/mL solution of dopamine HCl in 10 mM Tris-HCl (pH 8.5) for 30 minutes to form a thin polydopamine layer (5–50 nm) that provided a robust adhesive interface for subsequent covalent attachment of PEG-D [42]. The sensor was then rinsed with deionized water and dried with a nitrogen stream.

Next, 6 μL of 200 mg/mL of PEG-D in deionized water, 6 μL of 10 mM $NaIO_4$, and 12 μL of ethanol were combined onto the sensor surface and spun at 1000–1500 RPM for 3.75 minutes using a Chemat technology KW-4A spin coater. The oxidation of dopamine resulted in the solidification of PEG-D and chemically linked the PEG-D network to the polydopamine film through covalent crosslinking between the catechol moieties [43, 44]. The adhesive-coated sensors were dried and stored under vacuum until use. The presence of the PEG-D coating was verified by determining the change in mass and the resonant frequency before and after the coating process.

C. Characterization of the adhesive coating

The surface of the sensors was characterized using Fourier transform infrared (FTIR) spectroscopy (Perkin Elmer Spectrum One). The sensor was cut along its width to expose its cross-section and mounted onto a 90° cross-section holder to image its cross-section using field emission scanning electronic microscopy (FE-SEM, Hitachi S-4700). The average coating thickness was determined based on three measurements from at least three images.

D. Monitoring the degradation of the adhesive

The resonant frequency and amplitude of the ME sensors were determined before and after the PEG-D coating process using a custom magnetoelastic resonant sensor detector set to perform a frequency sweep from 150–165 kHz. The detector operated by applying an AC excitation field through a coil (100 turn, 4 cm long, 2 cm diameter) for 250 µs, followed by simultaneously disconnecting the excitation circuit and connecting to a detection circuit. Due to the stored energy in the sensor from the excitation stage, the magnetoelastic sensor continued to vibrate after the excitation signal was removed, and the response took the form of an exponentially decaying oscillation. The response of the decaying signal was determined using a comparator circuit with a known threshold and counting the number of threshold crossings, which was directly correlated to the damping of the sensor vibration. By repeating this process for a range of frequencies, the resonant frequency of the sensor was determined as the frequency that corresponded to the maximum number of threshold crossings. Furthermore, by monitoring a second predetermined threshold value, and applying the equation for an exponentially decaying function, the initial amplitude was calculated.

After initial characterization, the PEG-D coated ME sensors were placed in 2 ml vials containing acidic phosphate buffered saline (PBS) (pH5.7), neutral PBS (pH 7.4), or basic Tris-buffer (pH 10.0), followed by incubation at 37 °C to achieve thermal equilibrium. Three sensors were prepared for each pH. During the first week, each PEG-D coated ME sensor was interrogated three times a day using the custom ME box to track the dramatic mass changes of the PEG-D coating as a result of the adhesive swelling. The frequency of measurement was reduced to once a day after one week of incubation.

III. RESULTS AND DISCUSSION

An average of 0.64 ± 0.15 mg of dried adhesive was coated onto the sensor strips. The addition of the PEG-D reduced the resonant frequency of the sensors from 160.99 ± 0.67 kHz to 158.87 ± 1.08 kHz as a result of increased mass loading from the adhesive coating. The FTIR spectrum of Parylene-C-coated sensors revealed the presence of aromatic structures (3000, 2924 cm^{-1}; Figure 3). PEG-D-coated surfaces exhibited the presence of PEG ether bonds (1103 cm^{-1}, -C-O-C-), carbonyl group (1727 cm^{-1}, ester linkage), and alkyl group (2878 cm^{-1}, -CH$_2$-) peaks [38]. SEM images further confirmed the presence of the PEG-D coating (Figure 4). The thickness of the sensor was measured to be 29.8 ± 0.25 µm, which corresponds well with the reported thickness of 29 µm given by the manufacture. The thickness of the Parylene-C coating averaged around 8.6 ± 2.3 µm. The bottom layer of Parylene-C appeared to be delaminated from the sensor, which is likely an artifact resulting from cutting the sample to expose its cross-section for imaging. The average thickness of the dried PEG-D coating was measured to be 23.9 ± 4.4 µm. The FTIR spectrum of polydopamine-coated surface (data not shown) did not reveal new peaks potentially due to the extremely thin coating and its structure similarity when compared to the polyphenylic structure of Parylene-C. Similarly, the polydopamine coating was not visible using SEM imaging (data not shown).

Figure 5 plots the change in amplitudes of the PEG-D-coated ME sensors when they were incubated in pH 5.7, 7.4, and 10.0. As the coating degraded, the damping on the sensors decreased, which increased the magnitude of vibrations and hence the signal amplitudes at resonance. The degradation process of adhesive occurred rapidly when the sample was incubated in pH 10.0, as evident from the sharp increase in the curvature of plot that rapidly reaches saturation. In contrast, the curve for sensors in pH 5.7 increased slowly, pointing to a slower degradation process. To minimize the disturbance to the coated sensors, the buffer solutions were not changed during the experiment. Given the small amount of coated adhesive, the acidic degradation product (e.g., glutaric acid) was not expected to affect the pH of the buffer and the rate of degradation. The resonant frequencies of the sensor were also measured during the experiment; however, the changes in resonant frequencies were small compared to the frequency measurement resolution, thus only the resonant amplitude curves were used for analysis.

Results from Figure 5 suggest that both the Parylene-C and polydopamine coating layers remained attached to the sensor throughout testing. Delamination of the Parylene-C coating would have resulted in rapid sensor corrosion and a decrease in resonant amplitude. Similarly, delamination of the polydopamine layer would have resulted in a sharp rise in the measured amplitude data due to the detachment of a relatively large amount of PEG-D chemically tethered to polydopamine. Both of these occurrences were not observed. Most importantly, adhesive incubated in pH 5.7 was visibly attached to the sensor even after 80 days of incubation.

The curves in Figure 5 can be fitted with a function:

$$S = C + A \left(1 - e^{-bt} \right), \quad (1)$$

where S is the amplitude of the resonance, t is time in days, C is the starting voltage (at Day 1), A is the total change in amplitude after complete degradation of the sample, and b is the coefficient that describes the rate of degradation. Table 1 lists the coefficients of the curve fits for sensors at different pH.

The most important coefficient from the curve fits is b, which can be used to determine the degradation rate of the sample. By assuming that most coatings have been degraded when the degradation curves reach 90% of their final values ($S = 0.9A$), the degradation time for each sample can be predicted by solving Eq. (1) as:

$$t = \frac{-\ln(1 - 0.9)}{b} = 2.3/b \quad (2)$$

By substituting the b values in Table 1 into Eq. (2), the degradation times for samples at different pH can be predicted. Table 2 lists the predicted degradation times and the observed degradation times. The observed degradation times were determined by visually inspecting the test samples. The samples were considered to be completely degraded if there was no visible coating on them.

Table 2 shows that at pH 10.0, the PEG-D coating was expected to degrade by 34 days. Decreasing pH to 7.4 increases the degradation time to 68 days, and at pH 5.7 the degradation time is about 3 months. The predicted degradation times follow similar trends as observed from sample degradation. However, the observed degradation times were slightly lower than the predicted degradation times. This can be explained by inherent limitations of visual inspection, where the PEG-D coating appears to be gone but difficult to discern residue patches of coating persist unobserved on the sensor. In addition, the 90% cutoff point was set by assuming complete degradation of the sample even when about 10% of coating was still on the sensors.

The degradation experiment carried out at pH 7.4 is in agreement with previously reported data for PEG-D, which lost over 80% of its mass over 2 months [38]. However, it was challenging to quantify the mass of the adhesive toward the end of the degradation experiment using the traditional approach as the sample progressively became more fragile to handle. As such, it was difficult to determine the exact degradation time by following the mass of bulk hydrogel. The degradation behavior of PEG-D over a wide range of pH levels were also monitored and the rate of degradation increased with increasing pH as the hydrolysis rate of ester bonds occurs faster under basic conditions [45, 46]. Physiological pH varies with tissue type [6–8] and degree of blood oxygenation [9, 10] and thus it is critical to characterize the effect of pH on the rate of adhesive degradation. ME sensing technology reported here utilized significantly lower amount of adhesive ($\sim 10^3$ times lower) when compared to traditional approaches, making it a cost effective test to fully characterize the degradation behaviors of tissues adhesives under a wider range of physiological conditions.

Remote sensing technology reported here can potentially be futher engineered to track adhesive degradation *in vivo*. ME sensors have previously been utilitzed to characterize biointerfacial events in animal models [22, 41]. However, to implement this technology *in vivo*, numerous challenges may need to be addressed. One of which include the need to distinquish sensor responses associated with adhesive degradation from those associated with inflammatory response, dynamic motions, and mechanical forces present at the implantation site.

IV. CONCLUSIONS

A biomimetic PEG-D adhesive was coated onto ME sensor strips and the degradation behavior of the adhesive was monitored by tracking the resonant amplitude of the sensor. When the adhesive-coated sensors were incubated at pH 7.4 and 37°C, PEG-D degraded over a period of 2.5 months matching previous published results while using a significantly lower amount of adhesive. The degradation behavior of PEG-D also increased with incubation pH as the rate of ester bond hydrolysis increased. ME sensor strips remained functional over the entire time period as the coated adhesive underwent degradation in a wide range of pH levels, including most pH ranges that are physiologically relevant. The ME sensor platform investigated in this work provides a useful tool to characterize the degredation behavior of tissue adhesives in real time and paves the road toward developing a remote sensing technology for monitoring adhesive degradation *in vivo*.

Acknowledgments

References

1. Ikada, Y. Tissue adhesives. In: Chu, CC.; von Fraunhofer, JA.; Greisler, HP., editors. Wound Closure Biomaterials and Devices. Boca Raton, Florida: CRC Press, Inc.; 1997. p. 317-346.

2. Spotnitz, WD. History of tissue adhesive. In: Sierra, DH.; Saltz, R., editors. Surgical Adhesives and Sealants: Current Technology and Applications. Lancaster, Pennsylvania: Technomic Publishing Co. Inc.; 1996. p. 3-11.

3. Mehdizadeh M, Yang J. Design Strategies and Applications of Tissue Bioadhesives. Macromolecular Bioscience. 2013 Mar.13:271–288. [PubMed: 23225776]

4. Waugh, A.; Grant, A. Anatomy ans Physiology in Health and Illness. Churchill Livingstone Elsevier; 2010. The Blood.

5. Soller BR, Zhang S. Optical measurement of tissue pH for surgical and critical care monitoring. 1998:122–129.

6. Ohman H, Vahlquist A. In vivo studies concerning a pH gradient in human stratum corneum and upper epidermis. Acta Dermato-Venereologica. 1994; 74:375–379. [PubMed: 7817676]

7. Soller BR, Micheels RH, Coen J, Parikh B, Chu L, Hsi C. Feasibility of non-invasive measurement of tissue pH using near-infrared reflectance spectroscopy. Journal of Clinical Monitoring. 1996 Sep 01.12:387–395. 1996. [PubMed: 8934345]

8. Tannock IF, Rotin D. Acid Ph in Tumors and Its Potential for Therapeutic Exploitation. Cancer Research. 1989 Aug 15.49:4373–4384. [PubMed: 2545340]

9. Sims C, Seigne P, Menconi M, Monarca J, Barlow C, Pettit J, et al. Skeletal muscle acidosis correlates with the severity of blood volume loss during shock and resuscitation. Journal of Trauma-Injury Infection and Critical Care. 2001 Dec.51:1137–1145.

10. Soller BR, Khan T, Favreau J, Hsi C, Puyana JC, Heard SO. Investigation of muscle pH as an indicator of liver pH and injury from hemorrhagic shock. Journal of Surgical Research. 2003 Oct. 114:195–201. [PubMed: 14559446]

11. Liu Y, Zhan H, Skelton S, Lee BP. Marine Adhesive Containing Nanocomposite Hydrogel with Enhanced Materials and Bioadhesive Properties. MRS Proceedings. 2013; 1569:33–38.

12. Murphy JL, Vollenweider L, Xu F, Lee BP. Adhesive Performance of Biomimetic Adhesive-Coated Biologic Scaffolds. Biomacromolecules. 2010; 11:2976–2984. [PubMed: 20919699]

13. Anderson J, Lin M-H, Privette C, Flowers M, Murley M, Lee BP, et al. Wireless magnetoelastic sensors for tracking degradation profiles of nitrodopamine-modified poly(ethylene glycol). ScienceJet. 2015; 4:80.

14. Hernando A, Vazquez M, Barandiaran J. Metallic glasses and sensing applications. Journal of Physics E: Scientific Instruments. 1988; 21:1129.

15. Modzelewski C, Savage H, Kabacoff L, Clark A. Magnetomechanical coupling and permeability in transversely annealed Metglas 2605 alloys. Magnetics, IEEE Transactions on. 1981; 17:2837–2839.

16. O'handley, RC. Modern magnetic materials: principles and applications. In: O'Handley, Robert C., editor. Modern Magnetic Materials: Principles and Applications. Vol. 1. Wiley-VCH: 1999 Nov. p. 768ISBN 0-471-15566-7. 1999.

17. Grimes CA, Mungle CS, Zeng K, Jain MK, Dreschel WR, Paulose M, et al. Wireless magnetoelastic resonance sensors: a critical review. Sensors. 2002; 2:294–313.

18. Zourob M, Ong KG, Zeng K, Mouffouk F, Grimes CA. A wireless biosensor for the direct detection of organophosphorous pesticides. The Analyst. 2007; 132:338–343. [PubMed: 17554413]

19. Ong KG, Zeng K, Yang X, Shankar K, Ruan C, Grimes CA. Quantification of multiple bioagents with wireless, remote-query magnetoelastic micro-sensors. IEEE Sensors Journal. 2006; 6:514–523.

20. Roy SC, Ong KG, Zeng K, Grimes CA. Quantification of blood clotting kinetics II: Thromboelastograph analysis and measurement of erythrocyte sedimentation rate using magnetoelastic sensors. Sensor Letters. 2007 Jun.5:432–440.

21. Ong KG, Leland JM, Zeng K, Barrett G, Zourob M, Grimes CA. A rapid highly-sensitive endotoxin detection system. Biosensors and Bioelectronics. 2006; 21:2270–2274. [PubMed: 16356707]

22. Holmes HR, Tan EL, Ong KG, Rajachar RM. Fabrication of Biocompatible, Vibrational Magnetoelastic Materials for Controlling Cellular Adhesion. Biosensors. 2012; 2:57–69. [PubMed: 25585632]

23. Vlaisavljevich E, Holmes HR, Tan EL, Qian Z, Trierweiler S, Ong KG, et al. Magnetoelastic vibrational biomaterials for real-time monitoring and modulation of the host response. Journal of Materials Science: Materials in Medicine. 2013 Apr 01.24:1093–1104. 2013. [PubMed: 23354739]

24. Waite JH. Nature's underwater adhesive specialist. International Journal of Adhesion and Adhesives. 1987; 7:9–14.

25. Waite JH. Reverse engineering of bioadhesion in marine mussels. Annals of the New York Academy of Sciences. 1999; 875:301–309. [PubMed: 10415577]

26. Lee BP, Messersmith PB, Israelachvili JN, Waite JH. Mussel-Inspired Adhesives and Coatings. Annual Review of Materials Research. 2011; 41:99–132.

27. Lee, BP.; Dalsin, JL.; Messersmith, PB. Biomimetic adhesive polymers based on mussel adhesive proteins. In: Smith, AM.; Callow, JA., editors. Biological Adhesives. Vol. 2006. Berlin, Germany: Springer Berlin Heidelberg; p. 257-278.

28. Bilic G, Brubaker C, Messersmith PB, Mallik AS, Quinn TM, Haller C, et al. Injectable candidate sealants for fetal membrane repair: bonding and toxicity *in vitro* . American Journal of Obstetrics and Gynecology. 2010; 202:85.e1–85.e9. [PubMed: 20096254]

29. Haller CM, Buerzle W, Kivelio A, Perrini M, Brubaker CE, Gubeli RJ, et al. Mussel-mimetic tissue adhesive for fetal membrane repair: an ex vivo evaluation. Acta Biomaterialia. 2012 Dec. 8:4365–4370. [PubMed: 22885681]

30. Brodie M, Vollenweider L, Murphy JL, Xu F, Lyman A, Lew WD, et al. Biomechanical properties of Achilles tendon repair augmented with bioadhesive-coated scaffold. Biomedical Materials. 2011; 6:015014. [PubMed: 21266745]

31. Mehdizadeh M, Weng H, Gyawali D, Tang L, Yang J. Injectable citrate-based mussel-inspired tissue bioadhesives with high wet strength for sutureless wound closure. Biomaterials. 2012 Nov. 33:7972–7983. [PubMed: 22902057]

32. Brubaker CE, Kissler H, Wang L-J, Kaufman DB, Messersmith PB. Biological performance of mussel-inspired adhesive in extrahepatic islet transplantation. Biomaterials. 2010; 31:420–427. [PubMed: 19811819]

33. Hong S, Yang K, Kang B, Lee C, Song IT, Byun E, et al. Hyaluronic Acid Catechol: A Biopolymer Exhibiting a pH-Dependent Adhesive or Cohesive Property for Human Neural Stem Cell Engineering. Advanced Functional Materials. 2013; 23:1774–1780.

34. Kastrup CJ, Nahrendorf M, Figueiredo JL, Lee H, Kambhampati S, Lee T, et al. Painting blood vessels and atherosclerotic plaques with an adhesive drug depot. Proceedings of the National Academy of Sciences. 2012 Dec 11. 2012.

35. Dalsin JL, Hu BH, Lee BP, Messersmith PB. Mussel adhesive protein mimetic polymers for the preparation of nonfouling surfaces. Journal of the American Chemical Society. 2003; 125:4253. [PubMed: 12670247]

36. Pechey A, Elwood CN, Wignall GR, Dalsin JL, Lee BP, Vanjecek M, et al. Anti-adhesive coating and clearance of device associated uropathogenic escherichia coli cystitis. Journal of Urology. 2009; 182:1628–1636. [PubMed: 19683735]

37. Ko R, Cadieux PA, Dalsin JL, Lee BP, Elwood CN, Razvi H. Novel Uropathogen-Resistant Coatings Inspired by Marine Mussels. Journal of Endourology. 2008; 22:1153–1160. [PubMed: 18484883]

38. Liu Y, Meng H, Konst S, Sarmiento R, Rajachar R, Lee BP. Injectable Dopamine-Modified Poly(Ethylene Glycol) Nanocomposite Hydrogel with Enhanced Adhesive Property and Bioactivity. ACS Applied Materials & Interfaces. 2014; 6:16982–16992. [PubMed: 25222290]

39. Dalsin, JL.; Lee, BP.; Vollenweider, L.; Silvary, S.; Murphy, JL.; Xu, F., et al. Multi-armed Catechol Compound Blends. US Patent. 8,119,742. 2012.

40. Schwarz, JA.; Cristian, I.; Contescu; Karol; Putyera. Dekker Encyclopedia of Nanoscience and Nanotechnology. New York: M. Dekker; 2004. Biomedical Implants from Nanostructured Materials; p. 263-265.

41. Vlaisavljevich E, Janka L, Ong K, Rajachar R. Bioactive Magnetoelastic Materials as Coatings for Implantable Biomaterials. Journal of Medical Devices. 2009; 3:027528.

42. Shafiq Z, Cui J, Pastor-Pérez L, San Miguel V, Gropeanu RA, Serrano C, et al. Bioinspired Underwater Bonding and Debonding on Demand. Angewandte Chemie. 2012; 124:4408–4411.

43. Lee BP, Dalsin JL, Messersmith PB. Synthesis and Gelation of DOPA-Modified Poly(ethylene glycol) Hydrogels. Biomacromolecules. 2002; 3:1038–1047. [PubMed: 12217051]

44. Cencer MM, Liu Y, Winter A, Murley M, Meng H, Lee BP. Effect of pH on the rate of curing and bioadhesive properties of dopamine functionalized poly(ethylene glycol) hydrogels. Biomacromolecules. 2014; 15:2861–2869. [PubMed: 25010812]

45. Chao GT, Qian ZY, Huang MJ, Kan B, Gu YC, Gong CY, et al. Synthesis, characterization, and hydrolytic degradation behavior of a novel biodegradable pH-sensitive hydrogel based on polycaprolactone, methacrylic acid, and poly(ethylene glycol). Journal of Biomedical Materials Research Part A. 2008; 85A:36–46. [PubMed: 17688254]

46. van Dijk-Wolthuis WNE, van Steenbergen MJ, Underberg WJM, Hennink WE. Degradation kinetics of methacrylated dextrans in aqueous solution. Journal of Pharmaceutical Sciences. 1997; 86:413–417. [PubMed: 9109041]
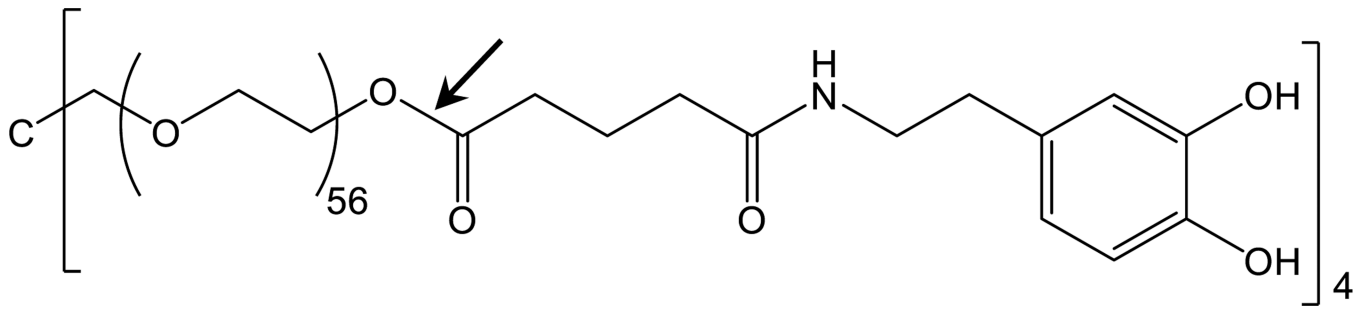
Figure 1.
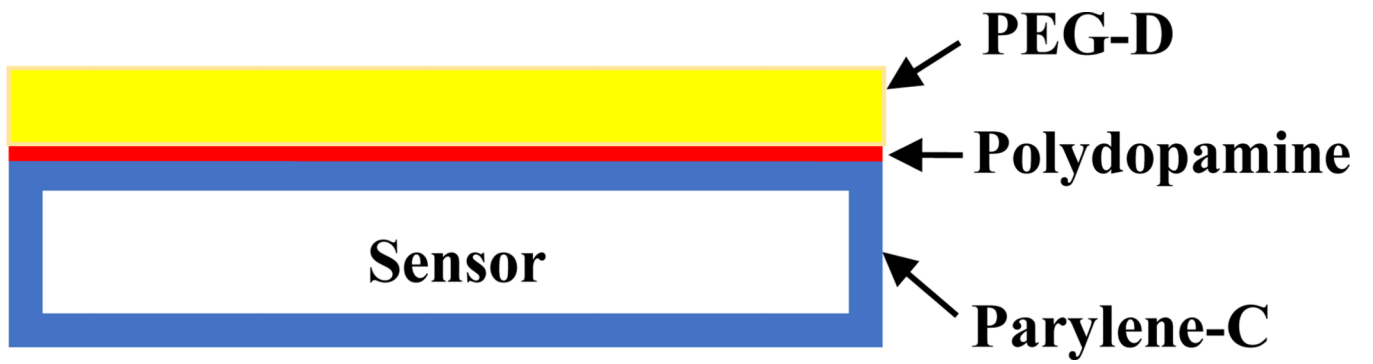Chemical structure of PEG-D. The arrow points to the hydrolysable ester linkage between PEG and glutaric acid.

Figure 2.
Schematic representation of a ME sensor coated with Parylene-C, polydopamine, and PEG-D.
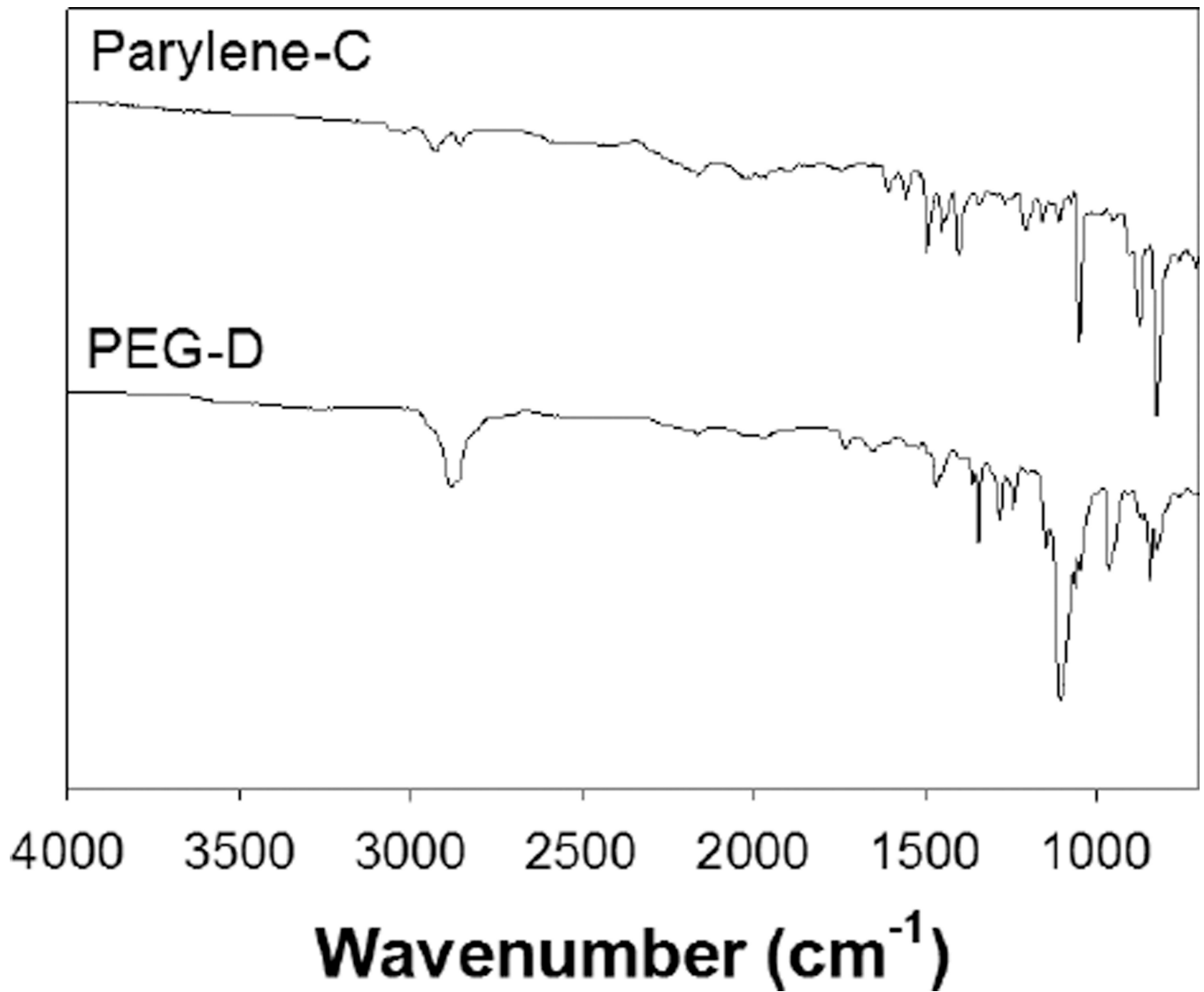
Figure 3.
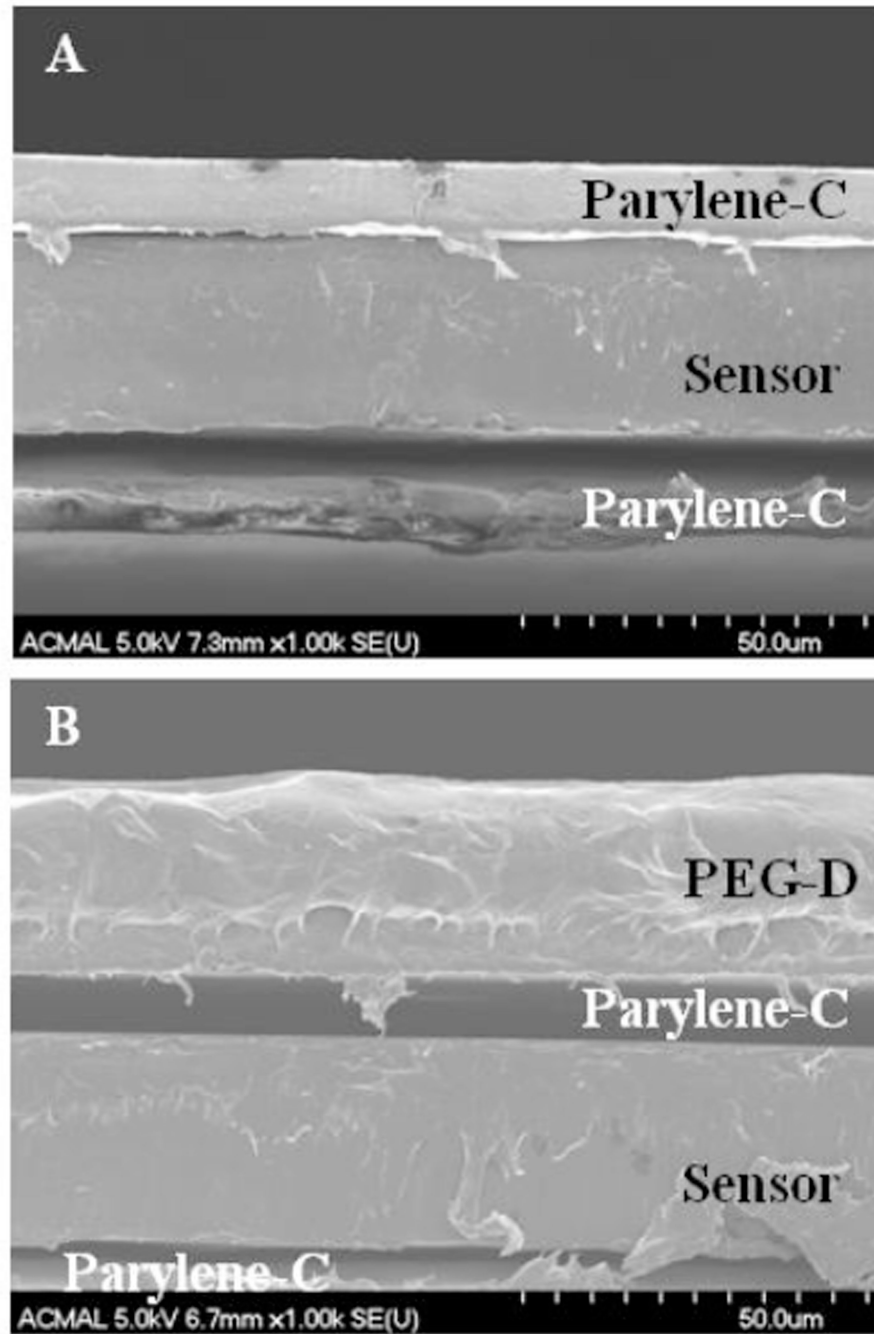FTIR spectra of Parylene-C- (top) and PEG-D-coated (bottom) sensors.

Figure 4.
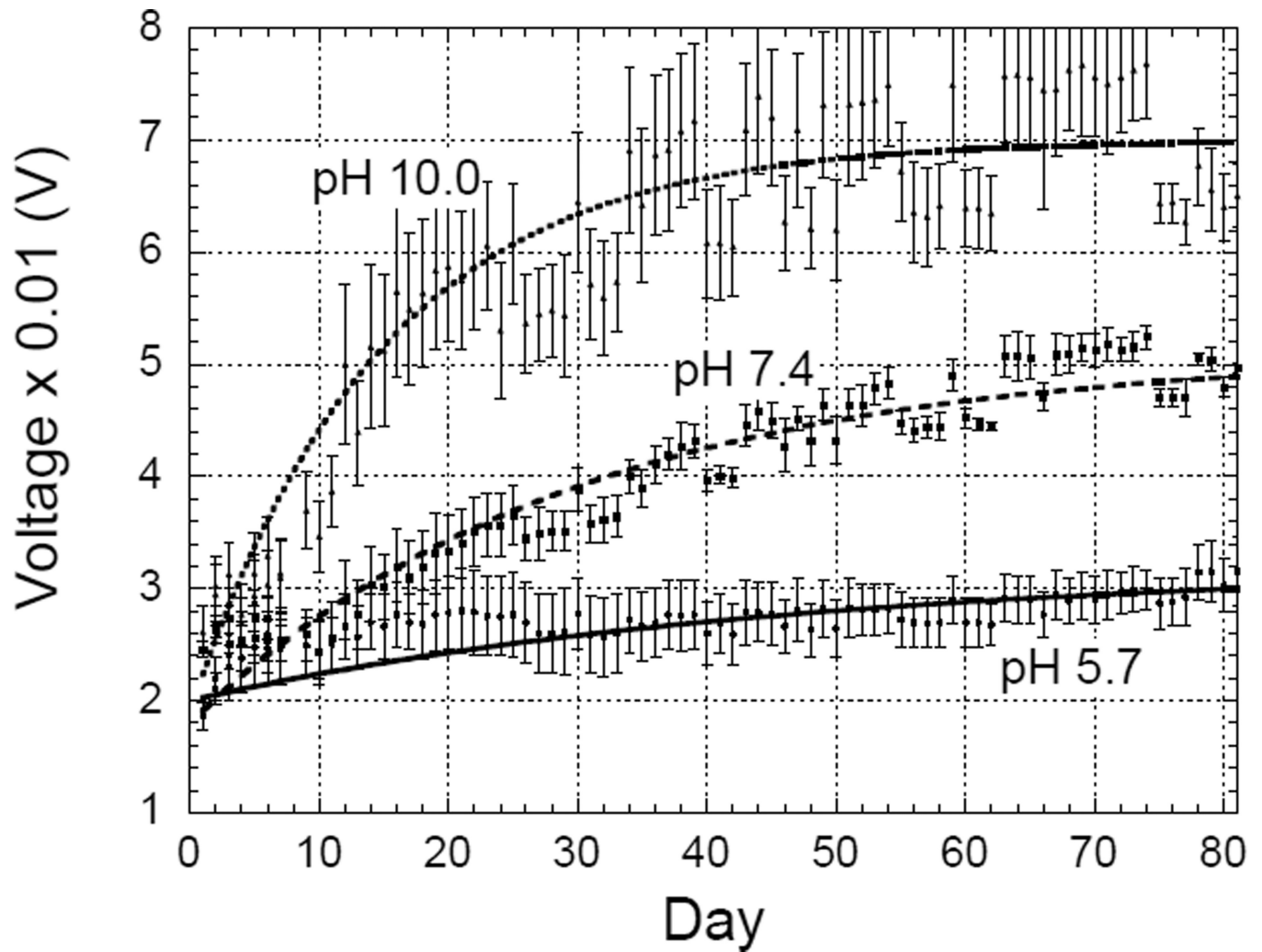SEM images Parylene-C- (**A**) and PEG-D-coated (**B**) sensors.

Figure 5.
Changes in the resonant amplitudes of PEG-D coated ME sensors incubated in pH 5.7, 7.4, and 10.0 at 37°C. The error bars for each pH represent the standard deviations of signals from 3 different sensors under the same testing conditions.

Table 1

Coefficients of the curves in Figure 4 fitted with Eq. (1).

pH	C	A	b
5.7	2.0	1.2	0.022
7.4	1.8	3.3	0.034
10.0	1.9	5.1	0.064

TABLE 2

The predicted and observed degradation times for sensors in different pH.

pH	Predicted Degradation Time	Observed Degradation Time
5.7	105	*
7.4	68	75
10.0	34	25

*The degradation time was not observed during the experimentation period.